

This document is confidential and is proprietary to the American Chemical Society and its authors. Do not copy or disclose without written permission. If you have received this item in error, notify the sender and delete all copies.

Molecular Determinants for the Activation/Inhibition of Bak Protein by BH3 Peptides

Journal:	<i>Journal of Chemical Information and Modeling</i>
Manuscript ID	Draft
Manuscript Type:	Article
Date Submitted by the Author:	n/a
Complete List of Authors:	Vila-Julià, Guillem; Polytechnic University of Catalonia, Department of Chemical Engineering; Universitat de Barcelona, Departament de Ciència dels Materials i Química Física Granadino-Roldan, Jose; Universidad de Jaen, Physical and Analytical Chemistry Perez, Juan Jesus; Universitat Politecnica de Catalunya, enginyeria química Rubio Martinez, Jaime; Universitat de Barcelona, Departament de Ciència dels Materials i Química Física

SCHOLARONE™
Manuscripts

Molecular Determinants for the Activation/Inhibition of Bak Protein by BH3 Peptides

Guillem Vila-Julià^{a,b}, José M. Granadino-Roldán^c, Juan J. Perez^b, Jaime Rubio-Martinez^{*a}

^a Department of Materials Science and Physical Chemistry, University of Barcelona and the Institut de Recerca en Química Teòrica i Computacional (IQTCUB), Barcelona, Spain

^b Department of Chemical Engineering. Universitat Politècnica de Catalunya- Barcelona Tech. Av. Diagonal, 647. 08028 Barcelona, Spain

^c Departamento de Química Física y Analítica, Facultad de Ciencias Experimentales, Universidad de Jaén, Campus "Las Lagunillas" s/n, 23071, Jaén, Spain

[†]Address correspondence to: Jaime Rubio-Martinez, Martí i Franques 1, E-08028 Barcelona, Spain. Phone: (+34) 93 4039263; Fax: (+34) 93 4021231; E-mail: jaime.rubio@ub.edu

Keywords: Apoptosis; Bcl-2 family; Molecular dynamics; MM-PB/GBSA approach; protein-protein interaction; Drug design.

Abstract

Apoptosis is a key procedure for all cells. Understanding this process and its regulation has been a subject of study in the last decades. Bcl-2 family of proteins are involved in the regulation of the apoptosis through the formation of homodimers or heterodimers between anti-apoptotic and pro-apoptotic proteins. Deregulation of pro-apoptotic proteins contributes to the progression of many tumour processes. Understanding how these proteins are activated is key to find new anti-cancer treatments. As no drug capable of activating Bak has been discovered yet, studying the structural and energetic insights of the binding of the known Bak activators, BH3 peptides, is essential to design new small molecules that resemble their binding to Bak. Recently, a BH3 Bim analogue has been discovered which inactivates Bak instead of activating it. Therefore, the present work is aimed to identify how BH3 peptides activate or inactivate Bak and determine any difference between them. Determination of the structural differences between the complexes with the activator and the inhibitor has been carried out by means of the study of the fluctuations of the corresponding Principal Components. Moreover, to calculate the binding free energy of the different complexes and to determine which residues of the peptide have the largest contribution to complex formation, MMPB/GBSA approaches are used. Results obtained in this work show differences in complexes with the activator and the inhibitor in structural and energetic terms, which can be used in the design of new molecules that could activate or inactivate pro-apoptotic Bak.

Introduction

Apoptosis is a form of programmed cell death indispensable for tissue homeostasis, embryonic development and immunity.¹ In this process, a cell undergoes a series of morphological transformations that lead to phagocytes recognition with its subsequent engulfment.² Deregulation of apoptosis has a major impact in disease. Thus, an excessive response to apoptosis signals can lead to an increased ischemic condition or drive neurodegeneration, whereas defective apoptosis has a major role in tumour development and autoimmune diseases, among others.³

Apoptosis is orchestrated by diverse cysteine proteases of the caspase family⁴ and is initiated through two different signalling pathways: the extrinsic and intrinsic pathways.¹ In the former, the process is mediated by cell surface death receptors that recognize specific signals from other cells and activate the caspase cascade, whereas in the latter, mitochondrial outer membrane permeabilization (MOMP) is produced as a consequence of cell stress or damage.^{1,5} MOMP facilitates the release of pro-apoptotic factors, such as cytochrome c, into the cytosol, triggering the assembly of the caspase-activating complex to initiate the activation of the executioner caspases 3, 6 and 7 for dismantling of the cell.^{1,5} This is a highly regulated process, since once MOMP is produced even if caspase activity is blocked, cells experience a bioenergetic collapse.^{6,7}

Members of the B-cell lymphoma-2 (Bcl-2) family of proteins are primary responsible for the control of the apoptotic intrinsic pathway, through the regulation of mitochondrial outer membrane permeability.^{8,9} These proteins share one or more specific conserved regions known as Bcl-2 homology (BH) domains, recognised to be crucial for function, as deletion of these domains via molecular cloning affects survival/apoptosis rates. Taking into account the number of BH domains they exhibit and their function in the apoptotic process (either pro-apoptotic or anti-apoptotic), these proteins can be classified into three groups. First, the anti-apoptotic or pro-survival Bcl-2 proteins (Bcl-2, Bcl-xL, Bcl-w, Mcl-1 and Bfl-1/A-1) that exhibit up to four BH-domains (BH1-BH4) and their role is to inhibit the activity of pro-apoptotic Bcl-2 proteins by binding them. Second, the pro-apoptotic effector Bcl-2 proteins (Bak and Bax), exhibiting also up to four BH domains (BH1-BH4), being the BH3-domain necessarily present for mitochondrial apoptosis signalling. These proteins are involved in mitochondrial outer membranes pore formation through homo-oligomerization. Third, the also pro-apoptotic BH3-only proteins (Bim, Bid, Puma, Bad, Bik, Bmf, Hrk, Noxa), sharing little sequence homology apart from the BH3-domain. This group can be further divided into two subgroups: the direct activators (Bim, Bid and Puma) that directly activate pro-apoptotic effectors, and the sensitizers (all BH3-only proteins), that indirectly activate Bak and Bax by binding to anti-apoptotic proteins and liberating the pro-apoptotic effectors. Some members of the family have also transmembrane domains at their C-terminus, which primarily function to localize them into the mitochondrial outer membrane.¹⁰

The interaction network between members of the Bcl-2 family is dominated by protein-protein interactions. Indeed, the elucidation of the molecular structure of diverse members and different BH3-domain–Bcl2 complexes has been key in recent years to understand MOMP regulation and provide novel opportunities for therapeutic intervention.^{11,12} All multi-BH domain members exhibit a conserved all- α globular structure that consists of nine α -helices (α 1– α 9) packed around helix α 5. The fold exhibits a *core* domain defined by helices α 2 – α 5 and a *latch* domain, defined by helices α 6 – α 8 (Figure 1) that is involved in the activation process. In the *core* domain, helices are packed in such a way that define a hydrophobic surface groove that is occupied by the C-terminus of the protein (α 9) when it is in its cytosolic form, but also is the site where the BH3-domain of other family members bind to.¹³ In contrast, most BH3-only proteins are intrinsically disordered, binding through the BH3-

1
2
3 domain into the hydrophobic groove of multi-BH domain members. Bid is the exception to this rule,
4 since it exhibits a multi-BH domain fold and requires cleavage to expose its BH3-domain, generating
5 the active form (truncated form or tBid).¹⁴
6

7
8 Bcl-2 proteins interact with each other generating a complicated interaction network that
9 regulates the apoptotic machinery. Despite knowledge accumulated in the last decades, our
10 understanding of the mechanism of this regulation is not yet complete.^{15,16} Thus, it is well established
11 that the relative concentrations of pro and anti-apoptotic proteins are a necessary condition that
12 determines cell commitment to undergo apoptosis. Thus, under normal conditions in healthy cells,
13 pro-survival Bcl-2 proteins sequester pro-apoptotic effectors as well as BH3-only proteins, preventing
14 apoptosis. However, upon a cytotoxic stimulus, the overwhelming number of BH3-only proteins
15 produced activate pro-apoptotic effectors either by direct binding or through the liberation of
16 restrained pro-apoptotic effectors by binding to pro-survival Bcl-2 proteins with the subsequent
17 MOMP induction to result in apoptosis.^{9,10} However, the variable affinities exhibited by the diverse
18 members of family for each other and their modulation when proteins are embedded in a membrane
19 are also relevant.¹⁰
20
21

22
23 In healthy cells, the pro-apoptotic effectors Bak and Bax are shuttled between the
24 mitochondria outer membrane and the cytosol at different rates.^{17,18} This differential behaviour makes
25 the former to be primarily attached to the mitochondria outer membrane through its C-terminus ($\alpha 9$),
26 whereas the latter is primarily found in the cytosol, adopting a globular form with its transmembrane
27 domain bound to its hydrophobic groove.¹⁷ Upon cytotoxic stress, Bak and Bax are accumulated and
28 activated at the mitochondrial outer membrane with their subsequent homo-oligomerization that
29 produces MOMP, a crucial event of intrinsic apoptosis. Accumulation of Bax in the mitochondrial outer
30 membrane is executed by an overwhelming number of BH3-only proteins produced after a cytotoxic
31 stress, some activating Bax and others, inhibiting pro-survival Bcl-2 proteins.
32
33

34
35 Crystallographic studies show that Bax exhibits two binding sites: the canonical hydrophobic
36 groove defined between helices $\alpha 2 - \alpha 5$ and a rear activation site, found between helices $\alpha 1$ and $\alpha 6$
37 at the opposite surface of the hydrophobic groove.¹⁹ BH3-only proteins interact with Bax at the rear
38 activation site, promoting the displacement of the loop between helices $\alpha 1$ and $\alpha 2$, which leads to the
39 displacement of its transmembrane domain from the hydrophobic groove, facilitating membrane
40 insertion.^{20,21} On the other hand, as Bak is constitutively inserted in the mitochondrial outer
41 membrane (MOM) through its $\alpha 9$ helix, the canonical hydrophobic groove was postulated as the only
42 activation site.^{20,22,23} However, it has recently been identified another activation site in the loop
43 between $\alpha 1$ and $\alpha 2$ triggered by antibodies.²⁴ Despite this apparent differential behaviour, there is
44 enough experimental evidence to support that they present conserved activation mechanisms.^{25,26}
45 Thus, the activation mechanism of these pro-apoptotic proteins once they are inserted in the MOM
46 consists in the transient binding of BH3-only proteins like Bim or tBid producing the dissociation of $\alpha 1$
47 from the $\alpha 6$ helix, and allowing the separation of the *latch* domain (helices $\alpha 6 - \alpha 8$) from the *core*
48 domain (helices $\alpha 2 - \alpha 5$). At this time, the affinity of the BH3-only protein decreases and Bak/Bax
49 exhibits fully exposed its BH3-domain to bind another Bak/Bax protein to produce symmetric dimers.
50 These dimers associate via $\alpha 6 : \alpha 6$ interface and further dimer-by-dimer homo-oligomers and form
51 macropores on the membrane triggering apoptosis.²⁷
52
53
54

55
56 The aim of this work is to analyse the structure of pro-apoptotic Bak and provide the molecular
57 determinants from the analysis of the complex with diverse BH3 peptides involved in the binding and
58 activation of Bak, such as Bid (EDIIRNIARHLAQVGDSDRSI) or Bim
59 (DMRPEIWIAQELRRIGDEFNAYYARR). The molecular determinants of a recently disclosed Bim
60 analogue are also analysed: Bim(h3Pc) (DMRPEIWIAQELRRXGDEFNAYYARR, where X = aminosuberic

acid)²⁸ which inhibits Bak, permitting to evaluate the structural and energetic differences that make it and inhibitor rather than an activator of Bak. A mutated form of Bid has also been analysed: BidAib₂ (EDIIRNIARHLAXVGDXMLRSI, where X = Aib), which has increased helicogenic residues, allowing to determine if an increased helical content can improve binding affinity. A non-globular conformation of Bak in complex with Bim²⁸ and with the inhibitor form of Bim are also studied to determine whether the interaction between Bak and the BH3-only peptide conserves the molecular determinants. These non-globular conformations are called *active* conformations, as they simulate the structure that are adopted when *latch* domain is separated from the *core* domain, in the initial steps during Bak activation. The results reported shed some light into a better understanding of the activation/inhibition mechanism of Bak and could be used for the development of novel activators/inhibitors of pro-apoptotic Bak to be translated into novel therapeutic agents.

Methods

Preparation of Bak/X Complexes

Three-dimensional structures of the Bak/Bim complex in its *active* state and of the Bak/Bid and Bak/Bim(h3Pc) complexes in their *inactive* state were retrieved from Protein Data Bank (PDB), with PDB codes 5VWV²⁸, 2M5B²⁹ and 5VWZ²⁸ respectively (Table S1, ESI). When needed, modifications to obtain the wild type (WT) sequence were performed for both Bak, Bim and Bid. The structure of the Bak/Bim complex in Bak *inactive* conformation was generated using the coordinates of the Bak/Bim(h3Pc) complex (PDB code 5VWZ).²⁸ The non-natural residue 155 (with residue name 9R1) was modified into its wild-type form: an Isoleucine, and missing atoms from this residue were completed using the *LEaP* module of the AMBER16 software.³⁰ Finally, the structure of the Bak/Bim(h3Pc) complex in Bak *active* conformation was generated from the Bak/Bim complex (PDB code 5VWV) where residue I155 of Bim was changed to the non-natural 9R1 residue.

Parameters for the h3Pc non-natural residue were obtained using distance, angles and dihedrals from glutamate, whilst missing parameters were obtained using the General Amber Force Field (gaff)³¹. Charges were generated with the restrained electrostatic potential (RESP) at HF/6-31G* level, which is the default charge approach applied in Amber protein force fields.^{31,32} The Bak/BidAib₂ complex has two special residues, the α -aminoisobutyric acid residues (Aib), which are used due to their strong helicogenic tendency, since they can promote helical folding in synthetic and natural sequences.^{33,34} This complex was used to determine whether the use of BH3 mimetic peptides with an increased helical content can improve binding affinity. Moreover, it is important to analyse if these residues have any implication in molecular determinants of the Bak/BH3 interaction. Parametrization of the residue Aib was obtained from *Bisetty et al.*³⁵

Molecular dynamics of Bak and Bak/X Complexes

All calculations reported in the present work were performed with the PMEMD (Particle Mesh Ewald Molecular Dynamics) code of the AMBER16 software in its CUDA version³¹ using the AMBER ff14SB force field.^{36,37}

Before performing molecular dynamics (MD) simulations, each system was first relaxed. Systems were soaked in a cubic box, using TIP3P³⁸ explicit water molecules with periodic boundary conditions. Minimizations were carried out stepwisely: first, positions of the water molecules and ions were optimized using the steepest descent (SD) algorithm³⁹ up to 5000 cycles of minimization, keeping fixed the rest of the system; in a second step, relaxation of the modelled residues was carried out in two stages, each one of 5000 cycles of SD, keeping fixed backbone positions of the modelled

residues and using a decreasing force constant of 5.0 and 0.1 kcal/Å; in the last step, the minimization of the whole system was carried out without any restrictions using 10000 cycles of SD method.

After minimization, systems were heated in steps of 30 K every 20 ps, maintaining all backbone atoms constrained with a force constant of 1.0 kcal/mol·Å. The heating process was performed under the canonical (NVT) ensemble. Once the systems were heated, a 200 ps simulation at constant pressure (NPT ensemble) was performed for density equilibration. The final structures were used as starting points for MD simulations. Trajectories were performed at 300 K by coupling the system to a thermal bath, using the Langevin thermostat.⁴⁰ All bonds involving hydrogen atoms were fixed using the SHAKE algorithm,⁴¹ which allowed us to use a time step of 2 fs in all the simulations. Non-bonded interactions were truncated using a cutoff of 9 Å, and long-range interactions were treated with the particle-mesh Ewald summation method.⁴² Three MD of 300 ns length were performed on each system to ensure their energy convergence and to enhance conformational sampling, but only the last 50 ns of each trajectory were considered for analysis. Sampling was carried out using multiple molecular dynamics trajectories, which results in a more thorough exploration of the conformational space reducing the chances the system gets trapped in a local minima.⁴³

Root-Mean Square Deviation (RMSD) and Root-Mean Square Fluctuation (RMSF)

Root-Mean Square Deviation (RMSD) along the simulation time was computed using the *cpptraj*⁴⁴ module from AMBER16 to assess the structural stability of the systems along the Molecular Dynamics simulation. RMSD was computed using the respective experimental structure obtained from LEaP, that is not minimized, as reference structure. Each of the frames of the diverse trajectories were reoriented over the residues from helices α_1 , α_3 , α_4 , α_5 and α_6 . Root-Mean Square Fluctuation (RMSF) for each of the residues of Bak and the diverse peptides were also computed using *cpptraj*. This provides information of the local conformational flexibility of each residue.

Principal Component Fluctuations

In order to determine and analyse the principal structural variations of the diverse systems studied, we computed the Principal Component Fluctuations of the most relevant secondary structures. For this purpose, we used the Principal Component Analysis (PCA), a multivariate statistical technique systematically applied to reduce the number of dimensions needed to describe protein dynamics through a decomposition process that describe motions from the largest to the smallest spatial scales. In this method, a covariance matrix constructed using the atomic coordinates of the alpha carbons ($C\alpha$) of every residue is diagonalized to produce a set of eigenvectors or Principal Components ($PC^{(i)}$, $i=1, N$, being N the number of residues of the protein), as well as their corresponding eigenvalues $\lambda^{(i)}$. Thus, this covariance matrix is a $3N \times 3N$ symmetric matrix. PCA transforms correlated variables into uncorrelated variables and once they are rank ordered, the first principal modes or eigenvectors can be used to characterize large-scale protein motions. In other words, these first modes are enough to define the “essential” space or motions of the protein.⁴⁵ The percent contribution of the i^{th} principal component $PC^{(i)}$, to the structural variance in the dataset is given by $c\% = 100 * \frac{\lambda^{(i)}}{\sum_{i=1}^{3N} \lambda^{(i)}}$, where the summation is performed over all $3N$ components. The square displacement of the k^{th} residue along the $PC^{(1)}$, $PC^{(2)}$... and $PC^{(n)}$ is:⁴⁶

$$PCF_{1 \leq i \leq n}^k = \text{tr} \left\{ \left[\sum_{i=1}^n \lambda^{(i)} PC^{(i)} PC^{(i)T} \right]_{kk} \right\}$$

where the square brackets represent a 3x3 submatrix of the full 3N x 3N matrix and the subscript kk stands for the kth diagonal element of this reduced submatrix. Results of this analysis provide the square summation of the fluctuations of the PCs (PCF) for residues of helices α_1 , α_2 , α_3 and α_5 and each PC fluctuation is computed using the current PC and all the previous PC cumulatively.

Binding Free Energy Calculations

Binding Free energies were computed using the Molecular Mechanics Poisson – Boltzmann Surface Area (MMPBSA) and the Molecular Mechanics Generalized - Born Surface Area (MMGBSA) algorithms,⁴⁷ implemented in the AMBER16 package. For both methods, free binding energy can be obtained according to the equation:

$$\Delta G_{binding} = \Delta H^{gas} + \Delta G^{solv} - T\Delta S^{gas}$$

where ΔH^{gas} is the gas-phase interaction energy calculated by summing the internal energy, the noncovalent van der Waals (ΔH_{vdW}^{gas}), and electrostatic (ΔH_{elec}^{gas}) molecular mechanics energies. On the other hand, ΔG^{solv} is computed as the sum of polar (ΔG_{polar}^{solv}) and non-polar terms ($\Delta G_{nonpolar}^{solv}$). ΔG_{polar}^{solv} can be calculated numerically by solving the Poisson-Boltzmann (PB) equation⁴⁸, or the simplified form, the Generalized Born (GB) method⁴⁹, for MMPBSA and MMGBSA algorithms, respectively. In the present work, we used the Onufriev-Bashford-Case (OBC) generalised Born method (igb=2)⁵⁰. Regarding to $\Delta G_{nonpolar}^{solv}$, it can be calculated using the following equation:

$$\Delta G_{nonpolar}^{solv} = \gamma SASA + \beta$$

where SASA is the Solvent-Accessible Surface Area, calculated using the LCPO method,⁵¹ and the values for γ and β constants were set to 0,00542 kcal/mol·Å² and 0,92 kcal/mol for MMPBSA⁵² and 0,0072 kcal/mol·Å² and 0 kcal/mol for MMGBSA⁵³. The entropic term was calculated within the harmonic entropy approximation using the normal-mode analysis with default values as implemented in the MMPBSA.py program⁵⁴. Because of the high computational requirements, the entropic contribution was averaged over 80 snapshots extracted at a time interval of 250 ps from the last 20 ns of each trajectory.

In the present work, binding free energies of the Bak/Bid, Bak/Bim, Bak/BidAib₂ and Bak/Bim(h3Pc) complexes were computed from three MD trajectories using MMPBSA and MMGBSA and the energy values were averaged over 50 ns after ensuring that each of these trajectories was stable.

Free Energy Decomposition

Contribution to the binding free energy of each of the residues of the BH3 peptides in each complex was analysed with the MMGBSA decomposition method⁵⁵ using the MMPBSA.py module of AMBER16. The procedure was carried out using the GB approach to calculate the electrostatic component of the solvation energy and LCPO for the nonpolar component. All energy components were calculated using the snapshots corresponding to the last 50 ns of each MD trajectory from each complex.

Analysis of Hydrogen Bonds

Hydrogen bonds between the Bak protein and the BH3 peptide ligands were also analysed using the *cptraj* module of AMBER16. The presence of these bonds was calculated over the last 50 ns of simulation time, and only hydrogen bonds with occupancies greater or equal to 60% were considered. Criteria used for hydrogen bonding was that the distance between the hydrogen-bond acceptor and the hydrogen-bond donor was lower than 3.0 Å and the angle between Acceptor – H – Donor more than 135°.

Clusterization

Similar structures for every complex were grouped into 10 different clusters using the *cptraj* module of AMBER16. This process was performed using the average link algorithm⁵⁶ and the backbone C α root-mean-square deviation of the superposed residues, the $\alpha 3$ and $\alpha 4$ helices involved in the interaction between Bak and the BH3 peptides, was used as a measure for the distance between two conformations

Results

As mentioned above, the aim of this study was to get a better understanding of the characteristics that allow the interaction between Bak and specific BH3 peptides (Bid, Bim, BidAib₂ and Bim(h3Pc)) and to analyse the structural and energy alterations that are taking place in all the systems. We have taken special interest in analysing the differences between Bak/Bim and Bak/Bim(h3Pc) complexes, being the former an activator of Bak and the latter an inhibitor, aiming at determining structural and energy differences that produce the change in activity.²⁸ We also wanted to analyse the differences between Bak/Bim and Bak/Bim(h3Pc) complexes on their *active* conformations, and determine if those differences that occur in the globular structures can be extrapolated in the *active* conformations, or in contrast, a different behaviour is observed. When analysing these results, structural and energy stability from different complexes were considered. Structural stability of each complex was calculated using the RMSD method and the analysis of the fluctuation has been performed with RMSF methods and with the analysis of the fluctuation of the Principal Components from the system. Binding free energy from these complexes was calculated using the MMPBSA and MMGBSA approaches. Moreover, detailed binding free energies from Bak residues were calculated using the free energy decomposition method.

Root-Mean Square Deviation and Root-Mean Square Fluctuation

RMSD was calculated along the trajectory to establish if the different MD simulations performed for every complex converge and are stable in structural terms. Residues superposed to perform these analyses were residues from helices $\alpha 3$, $\alpha 4$ and $\alpha 5$, involved in the binding of BH3-only peptides, and those from $\alpha 1$ and $\alpha 6$, which are relevant in the conformational changes that Bak experiences when it is activated. In the *active* conformations, $\alpha 6$ was not considered since it experiences an increase in its mobility due to its exposed conformation.

As it can be seen in Figure 2, the RMSD of the diverse Bak/BH3 peptide complexes experience an increase at the beginning of the trajectory, but after 50ns, all systems are structurally stabilized. When referring to the *active* conformations, they show a higher RMSD, as the *latch* domain is not

1
2
3 interacting with the *core* domain, and the globular structure moves to fill the space left by this *latch*
4 domain. RMSD for the Bak/Bid complex is slightly higher than that for the other globular
5 conformations. However, these differences are not as significant as those observed between *active*
6 and *inactive* conformations.
7
8

9 An analysis of the root-mean-square fluctuation (RMSF) per residue for the diverse complexes
10 (Figure 3), allows to conclude that all four globular complexes exhibit similar RMSF distributions,
11 showing a rigid behaviour in almost all the structure, with the $\alpha 1 - \alpha 2$ loop showing the largest
12 fluctuations. On the other hand, the *active* conformations show much higher fluctuation, due to the
13 movement of the *core* domain, which is trying to fill the space left from the *latch* domain.
14
15

16 Principal Component Fluctuation

17
18 The analysis of RMSF failed to identify differences between activators and the inhibitor in
19 structural terms. Thus, we decided to perform PCA, a powerful method to reveal the principal
20 variations in structure, studying the fluctuation of different residues (PCF). Figure 4 shows the
21 computed square summation of the atomic fluctuations for helices $\alpha 1$, $\alpha 2$, $\alpha 3$ and $\alpha 5$. As can be seen,
22 no differences between Bak/Bim and Bak/Bim(h3Pc) can be observed for residues of $\alpha 2$ and $\alpha 5$
23 (Figures 4B and 4D respectively). However, for the last residues of helix $\alpha 1$ (residues from 42 to 46)
24 (Figure 4A), the activator exhibits larger fluctuations in comparison to the inhibitor. This difference is
25 due to the interaction between residues 9R1 155 from Bim(h3Pc) and R42 from Bak, which is not found
26 in Bim wild type (WT). This difference in fluctuations may modify the structure of helix $\alpha 1$ as well as
27 the loop between $\alpha 1$ and $\alpha 2$, which is in close contact to $\alpha 6$, that is involved in the activation process
28 of Bak. As it can be seen, addition of more Principal Components does not improve the explanation of
29 the fluctuations of the system. Moreover, it was recently identified an activation site in this loop
30 triggered by antibodies.²⁴ Thus, if the inhibitor is decreasing the fluctuation of this region, it could be
31 affecting conformational changes that are necessary to produce a full activation of Bak.
32
33
34
35
36

37 Other differences between the activator and the inhibitor can be seen in diverse residues of
38 helix $\alpha 3$ (Figure 4C). In the complex with the activator, residues 87-92 experience large fluctuations,
39 whereas in the complex with the inhibitor these are found between residues 90-95. This difference is
40 due to the interaction between 9R1 155 from the inhibitor and N86, reducing the fluctuation at the
41 beginning of the helix. When Bak is on its *inactive* form, helix $\alpha 3$ is stabilized by the interaction
42 between D90 and R42. In the complex of Bak and the inhibitor, this interaction is being replaced by
43 the interaction of 9R1 155 of Bim(h3Pc) with R42, destabilizing helix $\alpha 3$.
44
45

46 The analysis of the fluctuation of the Principal Components of Bak/Bim and Bak/Bim(h3Pc) in
47 the *active* conformations show significant differences in regard to the *inactive* conformations (Figure
48 5). Large fluctuations can be seen in the whole structure as was observed in the RMSF analysis.
49 Fluctuation of residues of helix $\alpha 2$ shows no differences between Bak/Bim and Bak/Bim(h3Pc), as it
50 can be seen in Figure 5B, the same as observed in the *inactive* conformations. However, a large
51 fluctuation of residues in helix $\alpha 5$ is found in the Bak/Bim complex compared to the Bak/Bim(h3Pc)
52 one (Figure 5D). This increase of residue fluctuations is a consequence of the separation of the *latch*
53 domain from the *core* domain, since the absence of $\alpha 6$ produces an increase in the fluctuation to
54 occupy the free space. However, in this active conformation, the inhibitor form of Bim is fixing $\alpha 5$ helix
55 through its interaction with R137. This decreased fluctuation may be involved in the suppression of
56 later conformational changes needed for complete Bak activation.
57
58
59
60

1
2
3 Similar behaviour is experienced by residues from helix $\alpha 1$ of the Bak/Bim complex (see Figure
4 5A) in comparison to the Bak/Bim(h3Pc) complex, where larger fluctuations are observed in all the
5 residues and not only in the last as observed in the *inactive* conformations. In this case, in addition to
6 the interaction formed between Bak R42 and 9R1 155 from Bim(h3Pc), the separation of the *latch*
7 domain contributes to the increase in the fluctuation of helix $\alpha 1$ residues. As happened for helix $\alpha 5$,
8 this decreased fluctuation in the Bak complex with Bim(h3Pc) in comparison to the complex with the
9 WT form of Bim could affect conformational changes that take place later to fully activate Bak.
10
11

12
13 As shown in Figure 5C, residues of helix $\alpha 3$ fluctuate in both Bak/Bim and Bak/Bim(h3Pc)
14 complexes. However, the analysis of the average appearance frequency of hydrogen bonds between
15 Bak residues and 9R1 residue of Bim(h3Pc) in the *inactive* and *active* complexes (Table 1), reveals that,
16 in the *active* conformation, interaction between residue 9R1 155 from Bim(h3Pc) and N86 does not
17 occur with the same frequency as in the case of *inactive* conformation. Thus, the first residues from
18 helix $\alpha 3$ show a higher fluctuation in the *inactive* conformation than in the *active* from Bak/Bim(h3Pc)
19 complex. Focusing on the last residues of helix $\alpha 3$, fluctuation is slightly higher in Bak/Bim complex
20 than in Bak/Bim(h3Pc). This explanation could be contradictory with what it is seen in the *inactive*
21 conformation. However, in the *active* conformation from Bak/Bim complex, helix $\alpha 1$ is not stabilizing
22 helix $\alpha 3$, producing the increased fluctuation observed.
23
24
25

26 This difference is due to the interaction between 9R1 155 from the inhibitor and N86, reducing
27 the fluctuation at the beginning of the helix. When Bak is on its *inactive* form, helix $\alpha 3$ is stabilized by
28 the interaction between D90 and R42. In the complex of Bak and the inhibitor, this interaction is being
29 replaced by the interaction of 9R1 155 of Bim(h3Pc) with R42, destabilizing helix $\alpha 3$.
30
31

32 Binding Free Energy of the Complexes

33 Binding free energy was computed using MMPBSA and MMGBSA approaches for all the
34 complexes along the trajectory to determine the convergence of the different trajectories, their
35 stability in terms of binding energy and to carry out a more exhaustive analysis using the last
36 nanoseconds of the simulations. As it can be seen in Figures S1 and S2, the diverse complexes have
37 different $\Delta G_{\text{binding}}$ along the trajectory. Complexes between Bak and BH3 peptides have a similar
38 $\Delta G_{\text{binding}}$, with values between -90 and -100 kcal/mol. However, the Bak/Bim(h3Pc) complex exhibits a
39 more negative $\Delta G_{\text{binding}}$, around -140 kcal/mol. This increased $\Delta G_{\text{binding}}$ suggests a higher stability of the
40 complex, preventing the dissociation of the BH3 peptide from Bak.
41
42
43
44

45 Table 2 lists a detailed decomposition of the binding free energy computed using the MMPBSA
46 and the MMGBSA approaches for the diverse complexes using the last 50 ns of the corresponding MD
47 trajectories. As it can be seen, van der Waals contribution (ΔH_{vdw}) is notably important to favour
48 binding. It is important to mention that total electrostatic contribution ($\Delta H_{\text{ee}} + \Delta G_{\text{polar}}$), regardless of
49 the approach used, is unfavourable for the binding of all complexes, which underlines the importance
50 of the ΔH_{vdw} contribution. On the other hand, the entropic contribution to the binding energy is similar
51 for all the complexes studied. However, its contribution in the case of the inhibitor system,
52 Bak/Bim(h3Pc), is higher than the corresponding to the Bak/Bim activators, for both the *active* and
53 the *inactive* complexes. This suggests that the introduction of non-natural amino acids is not important
54 in terms of the entropic contribution to the binding energy.
55
56
57

58 The most significant result of these calculations is the higher binding free energy of the
59 Bak/Bim(h3Pc) complex in comparison to the rest. This difference is due to the presence of the 9R1
60

1
2
3 residue in Bim(h3Pc), which contributes to increase substantially the electrostatic term, which results
4 in this increased ΔG_{Total} . This phenomenon can be also observed in the *active* conformations, in which
5 Bim(h3Pc) total free binding energy is 20 kcal/mol higher than that of Bim. In the case of Bak/Bid and
6 Bak/Bim, the average binding free energy computed during the last 50 ns are similar. Similar values
7 for ΔG_{TOTAL} are obtained in the case of the Bak/BidAib₂ system, despite their increased helicogenity
8 due to the presence of the Aib residues.
9
10

11 When comparing *active* and *inactive* conformations without the entropic contribution, no
12 significant differences can be observed in the Bim complexes. In the case of the inhibitor Bim(h3Pc)
13 systems, the *inactive* conformation appears more stable. However, these trends are different when
14 the entropic contribution is included. In this case, when the inhibitor is bound, the two conformations
15 are similar; in contrast, for the activator there is a small difference between the two conformations.
16 Moreover, as shown in Figures S3 and S4, not only the Bak/Bim complex exhibits a similar energy
17 profile during all molecular dynamics simulations in both conformations, but also Bak/Bim(h3Pc)
18 exhibits a similar profile. Thus, despite the large difference in structural terms observed in the analysis
19 of RMSD, in energy terms these differences are more subtle, suggesting that the separation of the
20 *latch* domain from the *core* domain implies a small difference in the interaction between Bak and an
21 activator or an inhibitor and in this process the entropic changes can play a subtle role.
22
23
24
25

26 It is generally accepted that in the complexes formed between antiapoptotic and proapoptotic
27 proteins with BH3 peptides, the most relevant residues in terms of energy involved in the interaction
28 are hydrophobic. This observation is also seen in Figure 6 and Table S1, where for Bak bound to direct
29 activator BH3 peptides, the residues with higher energy contribution are mainly hydrophobic. The
30 exception is R127, whose contribution is mainly electrostatic due to it is involved in a hydrogen bond
31 with BH3 peptides (presence of this hydrogen bond, higher than 70% in all systems analysed). This
32 hydrogen bond not only occurs in the interaction between pro-apoptotic and BH3-only proteins, but
33 also in the interaction between anti-apoptotic and BH3-only proteins.⁵⁷
34
35
36

37 Comparison of the diverse free energy contributions per residue of the diverse complexes
38 with activators with those of the complex Bak/Bim(h3Pc), shows that some residues exhibit an
39 important contribution as a consequence of the I155X (X = suberic acid) mutation of Bim. This
40 mutation produces an approximation to residues of helices $\alpha 1$, $\alpha 3$ and $\alpha 5$ that were not reached by
41 the Isoleucine. These residues are R42, N86 and R137, which are establishing a hydrogen bond with
42 the 9R1 155 residue from Bim(h3Pc), as it can be seen in Figure 7. The frequency of the hydrogen
43 bonds involving this residue can be seen in Table 1.
44
45
46

47 This per residue free energy contribution is similar when comparing *inactive* and *active*
48 conformations, indicating that interactions that take place in the globular structure also take place in
49 the *active* conformations. Thus, the study of the interaction between BH3-only peptides with pro-
50 apoptotic proteins can be performed in the globular form, as it has been performed until nowadays,
51 without modifying the interaction pattern.
52
53

54 Pharmacophore Definition

55 In order to identify the stereochemical features that characterize the binding of different BH3
56 peptides, the most populated representative for each complex obtained from the clusterization of all
57 three MD simulations was used. Residues from the BH3-only peptides with the higher energy
58 contribution to the interaction have been used to design the pharmacophore. As it can be observed
59
60

1
2
3 in Figure 8, the pharmacophore is very similar in all complexes. BH3 peptides bind to the canonical
4 hydrophobic groove ($\alpha 3$, $\alpha 4$ and $\alpha 5$) of Bak primarily through hydrophobic features. A conserved
5 Hydrogen Bond interaction is present between Bak-R127 and BH3-D95/D157 (Bid and Bim
6 respectively). The mutated form of Bim, Bim(h3Pc), differs in the third hydrophobic feature, where
7 appears a Hydrogen Bond acceptor feature in the canonical hydrophobic groove, in a cavity from this
8 groove.
9
10

11
12 Analysis of the interaction between Bak and BH3-only proteins has always been performed in
13 the globular and *inactive* form of Bak. Thus, we wanted to analyse if there is any difference in the most
14 relevant features in the interaction when comparing this *inactive* form of Bak to its *active*
15 conformation. Results of distances and angles between these molecular features are shown in Figures
16 S5 and S6 and Tables S2 and S3. In these results it is clearly seen that there are no relevant differences
17 in the most important residues in the interaction between Bak/Bim and Bak/Bim(h3Pc) either in the
18 *active* or the *inactive* conformations. Thus, it confirms what was expected: if we want to find new
19 molecules that bind Bak, the study can be developed using the *active* or the *inactive* conformation
20 indistinctly.
21
22
23
24
25

26 Conclusions

27
28 Understanding the mechanism by which pro-apoptotic Bak is activated is a promising strategy
29 for designing an effective cancer therapy, as it develops a key role in the crucial process of apoptosis.
30 It is widely known that Bak remains inactivated in some diseases. Thus, the study of Bak structure and
31 interactions present in Bak protein complexes with BH3 peptides should give some perspective for
32 designing small molecules that can bind to Bak as other BH3-only proteins do. Moreover, inhibition of
33 Bak to prevent mitochondrial disruption may also be an effective strategy to inhibit cell death.
34
35

36
37 The analysis of the structural differences between Bak/Bim and Bak/Bim(h3Pc) showed that,
38 for globular or *inactive* structures, differences are present in helices $\alpha 1$ and $\alpha 3$, due to the interaction
39 formed between 9R1 residue of Bim(h3Pc) with R42 and N86 respectively. Fluctuation shift in the last
40 residues of $\alpha 1$ could explain the fact that conformational changes that take place during Bak activation
41 are being avoided. This conformational change is the dissociation of $\alpha 1$ helix from $\alpha 6$, which is needed
42 not only to separate the *latch* domain from the *core* domain, but also to form the apoptotic pore. On
43 the other hand, the different fluctuation between Bak/Bim and Bak/Bim(h3Pc) in $\alpha 3$ helix can be
44 explained by the interaction between 9R1 with N86, but also with the fact that the interaction
45 between 9R1 and R42 is competing with an intramolecular hydrogen bond between this arginine and
46 D90, from $\alpha 3$ helix, increasing the fluctuation of this helix in the inhibitor as seen in Figure 4C.
47
48
49

50
51 As the activation mechanism of Bak, and more accurately, the conformational changes that
52 Bak needs to experience to insert in the MOM are not fully understood, the analysis of an *active*
53 conformation of Bak has been performed. These *active* conformations resemble a posterior step of
54 Bak activation, where *latch* domain, helices $\alpha 6$ to $\alpha 8$, has been separated from the *core* domain,
55 helices $\alpha 2$ to $\alpha 5$. As all previous analyses of Bak had been performed using the globular structure, we
56 wanted to analyse if there are any differences in the interaction between *active* and *inactive*
57 conformations. In terms of structural differences, fluctuation is increased in overall structure, as the
58 separation of *latch* domain leaves an empty space, filled by the helices from the core domain.
59 However, this increase in the RMSF is not observed in helices $\alpha 1$ and $\alpha 5$, in which the interactions with
60

1
2
3 9R1 residue stabilize and decrease the movement of these helices. This reduction in the fluctuation is
4 showing that, despite the *latch* domain is already separated from the *core* domain, posterior
5 conformational changes in further Bak activation may be inhibited.
6

7
8 Moreover, we wanted to analyse Bak/Bim(h3Pc) complex on its *active* conformation to
9 determine the inactivation mechanism of this inhibitor. It has become clear that the inhibitor is
10 causing a difficulty in performing Bak conformational changes during activation. However, there is a
11 possibility that this inhibitor is also preventing Bak dimerization. Energetic analysis of the interaction
12 between Bak and BH3-only peptides has been carried out and it has been observed that the complex
13 with the inhibitor has a better free binding energy than with any other activators analysed. We have
14 hypothesized that this increase in the interaction indicates a higher difficulty in dissociate Bak from
15 BH3-only peptide, preventing the association of Bak-Bak by their BH3 domains. Nevertheless, to
16 assure this hypothesis, an analysis of the Bak-Bak interaction must be performed.
17
18

19
20 Predictions of binding free energy values are a key issue for determining the binding pattern
21 of a given molecule. These predictions are a complex issue, especially when structural data is obtained
22 from molecular dynamics simulations. Hence, two different approaches were used, MMPBSA and
23 MMGBSA, to have a proper performance when estimating binding free energy. Despite the expected
24 fluctuations observed in these predictions, both approaches and time intervals (last 50 ns of each MD
25 simulation) analysed lead to stability and equivalent results (Figures S1-S4).
26
27

28 Binding of BH3-only peptides to Bak protein is mainly conducted by hydrophobic interactions.
29 These hydrophobic features exist in BH3-only peptides conserved positions, confirming that BH3
30 domain is constituted of conserved hydrophobic residues in conserved positions. Residues from these
31 positions are: for Bid and BidAib₂, I86, L90, V93 and M97; and for Bim and Bim(h3Pc), I148, L152, I155
32 (9R1 for Bim(h3Pc)) and F159. Due to this major presence of hydrophobic features in the interaction
33 between Bak and BH3-only peptides, finding small selective molecules to activate Bak may signify an
34 increased difficulty.
35
36

37
38 It is true that hydrophobic interactions govern substantially the interaction between Bak and
39 BH3-only peptides. However, a hydrogen bond is present in all molecular dynamic simulations from
40 all complexes. This hydrogen bond, with R127 of Bak, is key in order to find more selective molecules
41 to activate Bak. Thus, it can be affirmed that although the binding of BH3-only proteins to Bak is mainly
42 hydrophobic, electrostatic interactions might also contribute to complex formation and increasing the
43 affinity of these proteins. Taking that into account, D157 in the case of Bim and D95 for Bid, has been
44 found critical for the interaction with R127 of Bak in all complexes. However, this interaction is not
45 only present in pro-apoptotic proteins, but it is also conserved in the interaction between BH3-only
46 proteins and antiapoptotic proteins. Therefore, this interaction is not specific of pro-apoptotic
47 proteins.
48
49

50
51 Analysis of the energy contribution by each residue was performed to determine the
52 differences in the interaction between Bak/Bim and Bak/Bim(h3Pc). While in Bak/Bim complex
53 interactions from the canonical hydrophobic groove are mainly hydrophobic, except for the hydrogen
54 bond between R127 and D157 of Bak and Bim respectively, in Bak/Bim(h3Pc) complex, this hydrogen
55 bond exists as well as the hydrophobic interactions. However, what increases affinity between Bak
56 and Bim and produces the already commented change of activity, inactivating Bak, is a hydrogen bond
57 formed between R42 or R137 from Bak and 9R1 residue from Bim(h3Pc).
58
59
60

1
2
3 Interaction between 9R1 and R42, R137 or N86 is really important for the activity switch of
4 Bak. Structural evidences in terms of fluctuation have demonstrated this importance. These evidences
5 are supported by the energetic results, which show an increased affinity for the inhibitor form. Thus,
6 this interaction helps decreasing the movement of these residues, which results in a more “fixed”
7 conformation.
8
9

10 All these changes that Bak suffers when is interacting with Bim(h3Pc) produce the previous
11 mentioned inactivation of Bak. As Bak structure and energetic terms are modified, two possibilities
12 arise that could inactivate Bak. On the one hand, as the movement of Bak is being altered, it could be
13 that what the inhibitor is doing is preventing conformational changes that take place during Bak
14 activation, which could be either the dissociation of the α 1 helix¹⁹ or the separation of *core* and *latch*
15 domain. As differences between Bak/Bim and Bak/Bim(h3Pc) also occur in the *active* conformations,
16 it could be that posterior conformational changes to fully activate Bak are also altered by the inhibitor.
17 On the other hand, as the affinity between Bak/Bim(h3Pc) is considerably higher than the one from
18 Bak/Bim complex, it is possible to assert that the dissociation of the inhibitor will be more difficult,
19 and the transient binding of BH3-only peptides would be more permanent, obstructing the
20 dimerization of Bak. In both possibilities the ability to permeabilize the MOM and to release
21 cytochrome c from the mitochondria is blocked, so apoptosis does not occur.
22
23
24
25

26 Pharmacophore features in the interaction between Bak and BH3-only peptides are nearly the
27 same when comparing *inactive* and *active* conformations. Only some differences in distances and
28 angles that involve residue 155, which is the one that varies, can be seen. However, these differences
29 are not significant, as it can be seen in Figures S5 and S6. Thus, it is possible to conclude that the
30 analysis of the interaction between Bak and BH3-only peptides can be performed in either the *inactive*
31 conformations, the way it has been performed so far, or the *active* conformation, with the *latch*
32 domain separated from the *core* domain, a more similar conformation when Bak is inserted in the
33 MOM.
34
35
36

37 Development of agents that are directly able to activate or inhibit Bak are important likewise:
38 further investigation in the activation of Bak by BH3 peptides is crucial to improve cancer therapy; and
39 inhibiting Bak might open many prospects to a better management of degenerative disorders.
40
41

42 Increasing knowledge about the activation mechanisms of pro-apoptotic proteins, and more
43 accurately, of Bak, is key to understand how cells develop the crucial process of apoptosis. Further
44 analysis and studies on Bak structure and on its interaction with BH3 peptides are needed, as well as
45 the study of Bak dimerization and oligomerization. Understanding how Bak is modified during its
46 activation and how it dimerizes and oligomerizes is essential in order to find new molecules that
47 simulate all these modifications and activate Bak in those cases that it is inactivated.
48
49

50 Acknowledgments

51 This study was supported by The Agència de Gestió d'Ajuts Universitaris i de Recerca (AGAUR)-
52 Generalitat de Catalunya (2017SGR1033). José M. Granadino-Roldán thanks the University of Jaén
53 (Acción 1 PIUJA 2017-2018) for financial support.
54
55
56

57 References

- 1
- 2
- 3
- 4 (1) Taylor, R. C.; Cullen, S. P.; Martin, S. J. Apoptosis: controlled demolition at the cellular level. *Nat. Rev. Mol. Cell Biol.* **2008**, *9*, 231-241.
- 5
- 6 (2) Elmore, S. Apoptosis: A Review of Programmed Cell Death, *Toxicologic Pathology*, **2007**, *35*, 495-
- 7 516.
- 8 (3) Favalaro, B.; Allocati, N.; Graziano, V.; Di Ilio, C.; De Laurenzi, V. Role of Apoptosis in disease, *Aging*,
- 9 **2012**, *4*, 330–49.
- 10 (4) Shalini, S.; Dorstyn, L.; Dawar, S.; Kumar, S. Old, new and emerging functions of caspases, *Cell Death*
- 11 *and Differentiation*, **2015**, *22*, 526-539.
- 12 (5) Tait, S. W. G.; Green, D. R. Mitochondria and cell death: outer membrane permeabilization and
- 13 beyond, *Nat. Rev. Mol. Cell Biol.*, **2010**, *11*, 621-632.
- 14 (6) Tait, S. W. G.; Parsons, M. J.; Llambi, F.; Bouchier-Haves, L.; Connel, S.; Muñoz-Pinedo, C.; Green,
- 15 D. R. Resistance to caspase-independent cell death requires persistence of intact mitochondria, *Dev.*
- 16 *Cell*, **2010**, *18*, 802-813.
- 17 (7) Kushnareva, Y.; Newmeyer, D. D. Bioenergetics and cell death, *Ann. NY Acad. Sci.*, **2010**, *1201*, 50-
- 18 57.
- 19 (8) Czabotar, P. E.; Lessene, G.; Strasser, A.; Adams, J. M. Control of apoptosis by the Bcl-2 protein
- 20 family: implications for physiology and therapy. *Nat. Rev. Mol. Cell Biol.*, **2014**, *15*, 49-63.
- 21 (9) Chipuk, J. E.; Moldoveanu, T.; Llambi, F.; Parsons, M. J.; Green, D. R. The Bcl-2 family reunion,
- 22 *Molecular Cell*, **2010**, *37*, 299-310.
- 23 (10) Singh, R.; Letai, A.; Sarosiek, K. Regulation of apoptosis in health and disease: the balancing act of
- 24 Bcl-2 family proteins. *Nature Reviews Molecular Cell Biology*, **2019**, *20*, 175-193.
- 25 (11) Delbridge, A. R.; Grabow, S.; Strasser, A.; Vaux, D. L. Thirty years of Bcl-2: translating cell death
- 26 discoveries into novel cancer therapies, *Nature Reviews Cancer*, **2016**, *16*, 99-109.
- 27 (12) Knight, T.; Luedtke, D.; Edwards, H.; Tauba, J. W.; Ge, Y. A delicate balance – The Bcl-2 family and
- 28 its role in apoptosis, oncogenesis and cancer therapeutics, *Biochemical Pharmacology*, **2019**, *162*, 250-
- 29 261.
- 30 (13) Kvensakul, M.; Hinds, M. G. The Bcl-2 family: structures, interactions and targets for drug
- 31 discovery, *Apoptosis*, **2015**, *20*, 136-150.
- 32 (14) Kvensakul, M.; Hinds, M. G. The Structural Biology of BH3-Only Proteins, *Methods Enzymol*, **2014**,
- 33 *544*, 49-74.
- 34 (15) Shamas-Din, A.; Kale, J.; Leber, B.; Andrews, D. W. Mechanisms of Action of Bcl-2 Family Proteins,
- 35 *Cold Spring Harb Perspect. Biol.*, **2013**, *5*, 1–21.
- 36 (16) Peña-Blanco, A.; García-Sáez, A. J. Bax, Bak and beyond - mitochondrial performance in apoptosis,
- 37 *The FEBS Journal*, **2018**, *285*, 416–431.
- 38 (17) Todt, F.; Cakir, Z.; Reichenbach, F. Emschermann, F.; Latuerwasser, J.; Kaiser, A.; Ichim, G.; Tait, S.
- 39 W. G.; Frank, S.; Langer, H. F.; Edlich, F. Differential retrotranslocation of mitochondrial Bax and Bak.
- 40 *The EMBO Journal*, **2015**, *34*, 67-80.
- 41 (18) Schellenberg, B.; Wang, P.; Keeble, J. A.; Rodriguez-Enriquez, R.; Walker, S.; Owens, T. W.; Foster,
- 42 F.; Tanianis-Hughes, J.; Brennan, K.; Streuli, C. H.; Gilmore, A. P. Bax Exists in a Dynamic Equilibrium
- 43 between the Cytosol and Mitochondria to Control Apoptotic Priming, *Molecular Cell*, **2013**, *49*, 959-
- 44 971.
- 45 (19) Gavathiotis, E.; Suzuki, M.; Davis, M. L.; Pitter, K.; Bird, G. H.; Katz, S. G.; Tu, H.-C.; Kim, H.; Cheng,
- 46 E. H.-Y.; Tjandra, N.; Walensky, L. D. Bax activation is initiated at a novel interaction site, *Nature*, **2008**,
- 47 *455*, 1076-1081.
- 48
- 49
- 50
- 51
- 52
- 53
- 54
- 55
- 56
- 57
- 58
- 59
- 60

- 1
2
3 (20) Alsop, A. E.; Fennell, S. C.; Bartolo, R. C.; Tan, I. K. L.; Dewson, G.; Kluck, R. M. Dissociation of Bak
4 α 1 helix from the core and latch domains is required for apoptosis, *Nature communications*, **2015**, 6,
5 1-13.
6
7 (21) Li, M. X.; Tan, I. K. L.; Ma, S. B.; Hockings, C.; Kratina, T.; Dengler, M. A.; Alsop, A. E.; Kluck, R. M.;
8 Dewson, G. BAK α 6 permits activation by BH3-only proteins and homooligomerization via the
9 canonical hydrophobic groove. *Proc. Natl. Acad. Sci. USA*. **2017**, 114, 7629-7634.
10
11 (22) Dai, H.; Smith, A.; Meng, X. W.; Schneider, P. A.; Pang, Y. P.; Kaufmann, S. H. Transient binding of
12 an activator BH3 domain to the Bak BH3-binding groove initiates Bak oligomerization, *J. Cell Biol.*,
13 **2011**, 194, 39-48.
14
15 (23) Brouwer, J. M.; Westphal, D.; Dewson, G. Robin, A. Y.; Uren, R. T.; Bartolo, R.; Thompson, G. V.;
16 Colman, P. M.; Kluck, R. M.; Czabotar, P. E. Bak core and latch domains separate during activation, and
17 freed core domains form symmetric homodimers, *Molecular Cell*, **2014**, 55, 938-946.
18
19 (24) Iyer, S.; Anwari, K.; Alsop, A. E.; Yuen, S. W.; Huang, D. C. S.; Carroll, J.; Smith, N. A.; Smith, B. J.;
20 Dewson, G.; Kluck, R. Identification of an activation site in Bak and mitochondrial Bax triggered by
21 antibodies, *Nature Communications*, **2016**, 7, 1-10.
22
23 (25) Moldoveanu, T.; Grace, C. R.; Llambi, F.; Nourse, A.; Fitzgerald, P.; Gehring, K.; Kriwacki, R. W.;
24 Green, D. R. BID-induced structural changes in BAK promote apoptosis, *Nature Structural and*
25 *Molecular Biology*, **2013**, 20, 589-597.
26
27 (26) Edlich, F. BCL-2 proteins and apoptosis: Recent insights and unknowns, *Biochem Biophys Res*
28 *Commun*, **2018**, 500, 26-34.
29
30 (27) Leschiner, E. S.; Braun, C. R.; Bird, G. H.; Walensky, L. D. Direct activation of full-length
31 proapoptotic Bak. *Proc. Natl. Acad. Sci. USA*, **2013**, 110, 963-995.
32
33 (28) Brouwer, J. M.; Lan, P.; Cowan, A. D.; Bernardini, J. P.; Birkinshaw, R. W.; van Delft, M. F.; Sleeb,
34 B. E.; Robin, A. Y.; Wardak, A.; Tan, I. K.; Reljic, B.; Lee, E. F.; Fairlie, W. D.; Call, M. J.; Smith, B. J.;
35 Dewson, G.; Lessene, G.; Colman, P.; Czabotar, P. M. Conversion of Bim-BH3 from activator to inhibitor
36 of Bak through structure-based design, *Molecular Cell*, **2017**, 68, 659-672.
37
38 (29) Wang, H.; Takemoto, C.; Akasaka, R.; Uchikubo-Kamo, T.; Kishishita, S.; Murayama, K.; Terada, T.;
39 Chen, L.; Liu, Z.-J.; Wang, B.-C.; Sugano, S.; Tanaka, A.; Inoue, M.; Kigawa, T.; Shirouzu, M.; Yokoyama,
40 S. Novel dimerization mode of the human Bcl-2 family protein Bak, a mitochondrial apoptosis
41 regulator. *Journal of Structural Biology*, **2009**, 166, 32-37.
42
43 (30) Case, D. A.; Betz, R. M.; Cerutti, D. S.; Cheatham, T. E., III; Darden, T. A.; Duke, R. E.; Giese, T. J.;
44 Gohlke, H.; Goetz, A. W.; Homeyer, N.; Izadi, S.; Janowski, P.; Kaus, J.; Kovalenko, A.; Lee, T. S.; LeGrand,
45 S.; Li, P.; Lin, C.; Luchko, T.; Luo, R.; Madej, B.; Mermelstein, D.; Merz, K. M.; Monard, G.; Nguyen, H.;
46 Nguyen, H. T.; Omelyan, I.; Onufriev, A.; Roe, D. R.; Roitberg, A.; Sagui, C.; Simmerling, C. L.; Botello-
47 Smith, W. M.; Swails, J.; Walker, R. C.; Wang, J.; Wolf, R. M.; Wu, X.; Xiao, L.; Kollman, P. A. (2016),
48 AMBER 2016, University of California, San Francisco.
49
50 (31) Wang, J.; Wolf, R. M.; Caldwell, J. W.; Kollman, P. A.; Case, D. A. Development and testing of a
51 General Amber Force Field, *J. Comput. Chem.*, **2004**, 25, 1157-1174.
52
53 (32) Bayly, C. I.; Cieplak, P.; Cornell, W. D.; Kollman, P. A. A well-behaved electrostatic potential based
54 method using charge restraints for deriving atomic charges: The RESP model, *J. Phys. Chem.*, **1993**, 97,
55 10269-10280.
56
57 (33) Aravinda, S.; Shamala, N.; Balaran, P. AiB residues in peptaibiotics and synthetic sequences:
58 analysis of nonhelical conformations, *Chemistry & Biodiversity*, **2008**, 5, 1238-1262.
59
60 (34) Delgado-Soler, L.; Orzaez, M. M.; Rubio-Martinez, J. Structure-based approach to the design of
BakBH3 mimetic peptides with increased helical propensity, *J. Mol. Model.*, **2013**, 19, 4305-4318.

- 1
2
3 (35) Bisetty, K.; Gomez-Catalan, J.; Aleman, C.; Giral, E.; Kruger, H. G.; Perez, J. J. Computational study
4 of the conformational preferences of the (R)-8-amino-
5 pentacyclo[5.4.0.0(2,6).0(3,10).0(5,9)]undecane-8-carboxylic acid mono-peptide, *J. Pept. Sci.*, **2004**,
6 10, 274-284.
- 7
8 (36) Maier, J. A.; Martinez, C.; Kasavajhala, K.; Wickstrom, L.; Hauser, K. E.; Simmerling, C. ff14SB:
9 Improving the accuracy of protein side chain and backbone parameters from ff99SB, *J. Chem. Theory*
10 *Comput.*, **2015**, 11, 3696-3713.
- 11
12 (37) Hornak, V.; Abel, R.; Okur, A.; Strockbine, B.; Roitberg, A.; Simmerling, C. Comparison of multiple
13 Amber force fields and development of improved protein backbone parameters. *Proteins* **2006**, 65,
14 712-725.
- 15
16 (38) Jorgensen, W. L.; Chandrasekhar, J.; Madura, J. D.; Impey, R. W.; Klein, M. L. Comparison of simple
17 potential functions for modeling water. *J. Chem. Phys.* **1983**, 79, 926-935.
- 18
19 (39) Arfken, G. B.; Weber, H. J. *Mathematical Methods for Physicists*, Elsevier Academic Press, 6th
20 edition, 2005, Method of Steepest Descents, 489-497.
- 21
22 (40) Allen, M. P.; Tildesley, D. J. *Computer Simulation of Liquids*, Oxford University Press, New York,
23 2017.
- 24
25 (41) Ryckaert, J. P.; Ciccotti, G.; Berendsen, H. J. C.; Numerical integration of the cartesian equations
26 of motion of a system with constraints: molecular dynamics of n-alkanes, *J. Comput. Phys.*, **1977**, 23,
27 327-341.
- 28
29 (42) Darden, T.; York, D.; Pedersen, L. Particle mesh Ewald-anN.Log(N) method for Ewald sums in large
30 systems, *J. Chem. Phys.*, **1993**, 98, 10089-10092.
- 31
32 (43) Perez, J. J.; Tomas, M. S.; Rubio-Martinez, J. Assessment of the sampling performance of multiple-
33 copy dynamics versus a unique trajectory. *J. Chem. Inf. Model.* **2016**, 56, 1950-1962.
- 34
35 (44) Roe, D. R.; Cheatham T. E. PTRAJ and CPPTRAJ: Software for processing and analysis of molecular
36 dynamics trajectory data, *J. Chem. Theory Comput.*, **2013**, 9, 3084-3095.
- 37
38 (45) Amadei, A. Linssen, A. B.; Berendsen, H. J. Essential dynamics of proteins, *Proteins*, **1993**, 17, 412-
39 425.
- 40
41 (46) Bakan, A.; Bahar, I. The intrinsic dynamics of enzymes plays a dominant role in determining the
42 structural changes induced upon inhibitor binding, *Proc. Natl. Acad. Sci. USA*, **2009**, 106, 14349-14354.
- 43
44 (47) Kollman, P. A.; Massova, I.; Reyes, C.; Kuhn, B.; Huo, S.; Chong, L.; Lee, M.; Lee, T.; Duan, Y.; Wang,
45 W.; Donini, O.; Cieplak, P.; Srinivasan, J.; Case, D. A.; Cheatham, T. E. Calculating structures and free
46 energies of complex molecules: Combining molecular mechanics and continuum models, *Acc. Chem.*
47 *Res.*, **2000**, 33, 889-897.
- 48
49 (48) Luo, R.; David, L.; Gilson, M. K. Accelerated Poisson-Boltzmann calculations for static and dynamic
50 systems, *J. Comput. Chem.*, **2002**, 23, 1244-1253.
- 51
52 (49) Tsui, V.; Case, D. A. Theory and applications of the generalized born solvation model in
53 macromolecular simulations, *Biopolymers*, **2000**, 56, 275-291.
- 54
55 (50) Onufriev, A.; Bashford, D.; Case, D. A. Exploring protein native states and large-scale
56 conformational changes with a modified generalized born model, *Proteins*, **2004**, 55, 383-394.
- 57
58 (51) Weiser, J.; Shenkin, P. S.; Still, W. C. Approximate solvent-accessible surface areas from
59 tetrahedrally directed neighbour densities, *Biopolymers*, **1999**, 50, 373-380.
- 60
61 (52) Kuhn, B.; Gerber, P.; Shulz-Gasch, T.; Stahl, M. Validation and use of the MM-PBSA approach for
62 drug discovery, *J. Med. Chem.*, **2005**, 48, 4040-4048.
- 63
64 (53) Gohlke, H.; Case, D. A. Converging free energy estimates: MMPB(GB)SA studies on the protein-
65 protein complex Ras-Raf. *J. Comput. Chem.*, **2004**, 25, 238-250.

1
2
3 (54) Miller, B. R.; McGee, T. D.; Swails, J. M.; Homeyer, N.; Gohlke, H.; Roitberg, A. E. MMPBSA.py: an
4 efficient program for end-state free energy calculations. *J. Chem. Theory Comput.*, **2012**, 8, 3314–
5 3321.
6

7 (55) Gohlke, H.; Kiel, C.; Case, D. A. Insights into protein-protein binding by binding free energy
8 calculation and free energy decomposition for the Ras-Raf and Ras-RalGDS complexes. *J. Mol. Biol.*,
9 **2003**, 330, 891-913.
10

11 (56) Rokach, L.; Maimon, O. *Data Mining and Knowledge Discovery Handbook*, Maimon, O. Rokach, L.,
12 Springer, Boston, MA, 2005, Clustering Methods, 321-352.
13

14 (57) Delgado-Soler, L.; Pinto, M.; Tanaka-Gil, K.; Rubio-Martinez, J. Molecular Determinants of
15 Bim(BH3) peptide binding to pro-survival proteins, *J. Chem. Inf. Model.*, **2012**, 52, 2107-2118.
16
17
18
19
20
21
22
23
24
25
26
27
28
29
30
31
32
33
34
35
36
37
38
39
40
41
42
43
44
45
46
47
48
49
50
51
52
53
54
55
56
57
58
59
60

Table 1: Average frequency appearance of hydrogen bonds in the last 50ns of all simulations between Bak residues and 9R1 155 residue from Bim(h3Pc) in the *inactive* and *active* complexes.

H-BOND	<i>INACTIVE</i>		<i>ACTIVE</i>	
	Frequency (%)	Average (%)	Frequency (%)	Average (%)
ARG 42 (NH1) - 9R1 155	96.4		96.4	
	98.2	97.0	98.2	97.0
	96.3		96.3	
ARG 42 (NH2) - 9R1 155	95.3		96.9	
	97.5	96.4	97.7	97.7
	96.3		98.6	
ARG 137 (NE) - 9R1 155	73.9		88.4	
	92.7	79.6	87.9	84.6
	72.1		77.5	
ARG 137 (NH2) - 9R1 155	92.3		70.9	
	30.5	69.4	88.1	83.8
	85.3		92.5	
ASN 86 (ND2) - 9R1 155	75.0		0	
	79.5	77.3	0	0
	77.3		0	

Table 2. Contribution of the different energy terms and total binding free energies (kcal/mol) for the different Bak-X complexes (X= Bid, BidAib2, Bim, Bim(h3Pc), Bim (active) and Bim(h3Pc) (active)) obtained by MMPBSA and MMGBSA in the last 50 ns of molecular dynamics. Final binding energy in bold. Standard deviation of the mean is shown.

	Bid	BidAib₂	Bim	Bim(h3Pc)	Bim (active)	Bim(h3Pc) (active)
ΔH_{vdW}	-102.8 ± 0.1	-111.1 ± 0.0	-125.4 ± 0.1	-134.0 ± 0.2	-124.1 ± 0.1	-125.3 ± 0.1
ΔH_{ee}	-172.0 ± 0.6	-143.6 ± 0.3	-181.3 ± 0.4	-246.4 ± 0.7	-160.6 ± 1.0	-156.8 ± 0.7
$\Delta G_{\text{polar,PB}}$	192.4 ± 0.5	178.3 ± 0.2	218.2 ± 0.3	252.1 ± 0.6	197.1 ± 1.0	165.0 ± 0.6
$\Delta G_{\text{nonpolar,PB}}$	-11.6 ± 0.0	-13.2 ± 0.0	-14.7 ± 0.0	-15.6 ± 0.0	-14.0 ± 0.0	-14.4 ± 0.0
$\Delta G_{\text{polar,GB}}$	200.0 ± 0.5	178.3 ± 0.2	219.0 ± 0.4	254.8 ± 0.6	199.3 ± 0.9	168.7 ± 0.6
$\Delta G_{\text{nonpolar,GB}}$	-13.9 ± 0.0	-13.9 ± 0.0	-17.4 ± 0.0	-20.0 ± 0.0	-16.8 ± 0.0	-18.7 ± 0.0
$\Delta G_{\text{PB,Total}}$	-94.1 ± 0.1	-89.6 ± 0.1	-103.2 ± 0.1	-143.8 ± 0.0	-101.6 ± 0.1	-131.5 ± 0.2
$\Delta G_{\text{GB,Total}}$	-88.8 ± 0.0	-90.3 ± 0.1	-105.1 ± 0.1	-145.5 ± 0.1	-102.1 ± 0.2	-132.1 ± 0.2
- TΔS	45.2 ± 0.1	43.5 ± 0.1	54.9 ± 0.1	63.9 ± 0.1	44.7 ± 0.1	53.7 ± 0.2
$\Delta G_{\text{binding_PB}}$	-48.9 ± 0.2	-46.1 ± 0.2	-48.3 ± 0.2	-79.9 ± 0.1	-56.8 ± 0.2	-77.9 ± 0.4
$\Delta G_{\text{binding_GB}}$	-43.6 ± 0.1	-46.8 ± 0.2	-50.2 ± 0.2	-81.6 ± 0.2	-57.4 ± 0.3	-78.4 ± 0.4

Caption for Figures

Figure 1: Crystal structure of Bak in complex with a BH3-only peptide. *Core* domain is formed by helices $\alpha 2$, $\alpha 3$, $\alpha 4$ and $\alpha 5$, and *latch* domain is formed by $\alpha 6$, $\alpha 7$ and $\alpha 8$. Full length pro-apoptotic Bak has 9 α -helices but $\alpha 9$, which is the transmembrane helix, has not been crystalized. (A) Bak on its soluble or globular form in complex with a BH3-only peptide. (B) Bak in complex with a BH3-only peptide in a conformation of the early activation steps, with the two domains, *core* and *latch*, separated.

Figure 2: Average Root-Mean Square Deviation (\AA) of three molecular dynamics simulations as a function of time from backbone atoms in the complexes between Bak and BH3-only peptides. In red, Bak complex with Bid; in blue in complex with BidAib₂; in green with Bim; and in yellow, Bim(h3Pc). Active conformations from Bim and Bim(h3Pc) are represented in grey and orange, respectively.

Figure 3: Average Root-Mean Square Fluctuation (\AA^2) from backbone atoms of three molecular dynamics simulations as a function of Bak residues in the complexes between Bak and BH3-only peptides. In red, Bak complex with Bid; in blue in complex with BidAib₂; in green with Bim; and in yellow, Bim(h3Pc). Active conformations from Bim and Bim(h3Pc) are represented in grey and orange, respectively.

Figure 4: Principal Component Fluctuation (\AA^2) from Bak residues in the globular form. In red, fluctuation of Bak residues in complex with Bim, and in blue, fluctuation of Bak residues in complex with Bim(h3Pc). In both cases, each Principal Component (PC) illustrates the square summation of the PCs of residues and all the previous ones. (A) Square summation of all atoms fluctuation from helix $\alpha 1$. (B) Square summation of the fluctuation from all residues from helix $\alpha 2$. (C) Square summation of all residues fluctuation from helix $\alpha 3$. (D) Square summation of the fluctuation from all residues from helix $\alpha 5$.

Figure 5: Principal Component Fluctuation (\AA^2) from Bak residues in the active conformations. In red, fluctuation of Bak residues in complex with Bim, and in blue, fluctuation of Bak residues in complex with Bim(h3Pc). In both cases, each Principal Component (PC) illustrates the square summation of the PCs of residues and all the previous ones. (A) Square summation of all atoms fluctuation from helix $\alpha 1$. (B) Square summation of the fluctuation from all residues from helix $\alpha 2$. (C) Square summation of all residues fluctuation from helix $\alpha 3$. (D) Square summation of the fluctuation from all residues from helix $\alpha 5$.

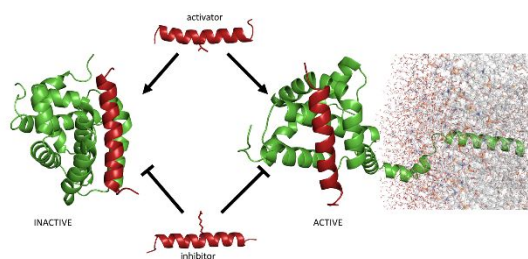
Figure 6: Average Total ΔG (kcal/mol) from Bak residues of three molecular dynamics simulations in the complexes between Bak and BH3-only peptides. In red, Bak complex with Bid; in blue, in complex with BidAib₂; in green, with Bim; and in yellow, Bim(h3Pc). Active conformations from Bim and Bim(h3Pc) are represented in grey and orange, respectively.

1
2
3 Figure 7: Interaction site from residue 9R1 155 from Bim(h3Pc). Pro-apoptotic protein Bak is
4 represented in green and BH3 peptide Bim(h3Pc) in blue. Residues from Bak involved in the hydrogen
5 bond with 9R1 are R42, N86 and R137.
6
7
8

9
10 Figure 8: Pharmacophore representation of the interaction between Bak and BH3-only peptides Bim
11 and Bim(h3Pc) on its inactive and active conformations. Light grey and light red are used for molecular
12 features of the inactive conformations, while dark grey and dark red are used for features in the active
13 conformations. (A) Comparison between Bak/Bim complexes on its inactive and active form. (B)
14 Comparison between Bak/Bim(h3Pc) complexes on its inactive and active form.
15
16
17
18
19
20
21

22 Table of Contents

23
24



25
26
27
28
29
30
31
32
33
34 Molecular determinants for the activation/inhibition of Bak protein on its active/inactive
35 conformation by BH3 peptides.
36
37
38
39
40
41
42
43
44
45
46
47
48
49
50
51
52
53
54
55
56
57
58
59
60

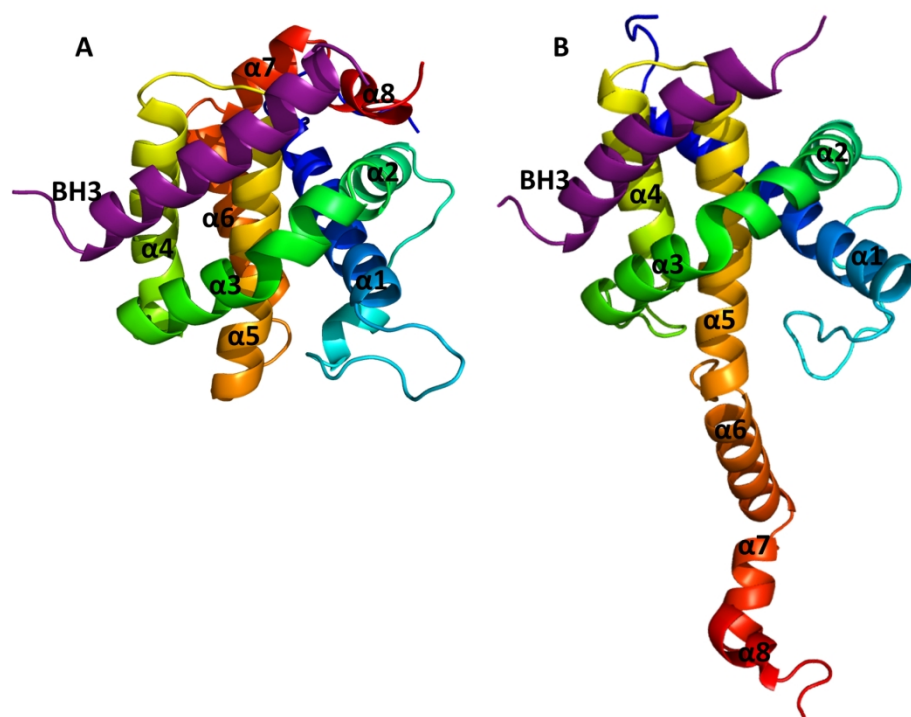


Figure 1: Crystal structure of Bak in complex with a BH3-only peptide. Core domain is formed by helices α_2 , α_3 , α_4 and α_5 , and latch domain is formed by α_6 , α_7 and α_8 . Full length pro-apoptotic Bak has 9 α -helices but α_9 , which is the transmembrane helix, has not been crystallized. (A) Bak on its soluble or globular form in complex with a BH3-only peptide. (B) Bak in complex with a BH3-only peptide in a conformation of the early activation steps, with the two domains, core and latch, separated.

170x129mm (300 x 300 DPI)

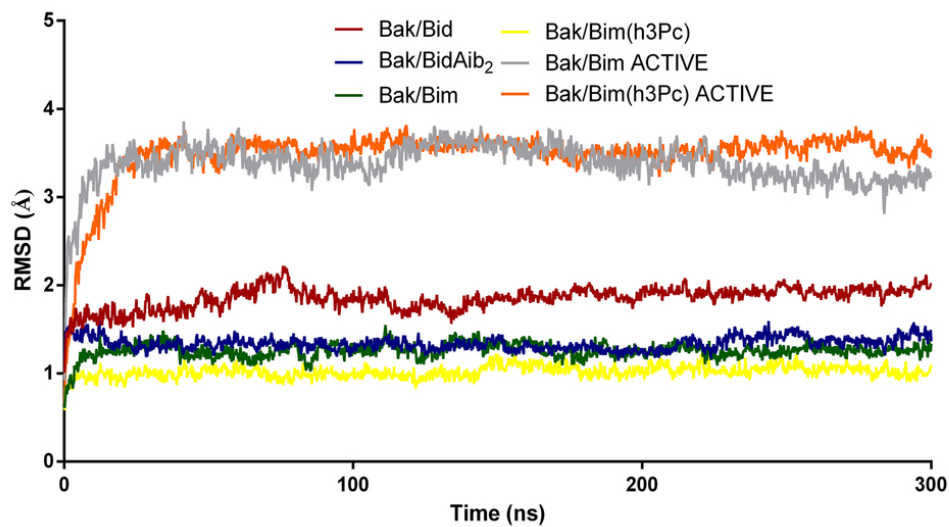


Figure 2: Average Root-Mean Square Deviation (\AA) of three molecular dynamics simulations as a function of time from backbone atoms in the complexes between Bak and BH3-only peptides. In red, Bak complex with Bid; in blue in complex with BidAib₂; in green with Bim; and in yellow, Bim(h3Pc). Active conformations from Bim and Bim(h3Pc) are represented in grey and orange, respectively.

82x45mm (300 x 300 DPI)

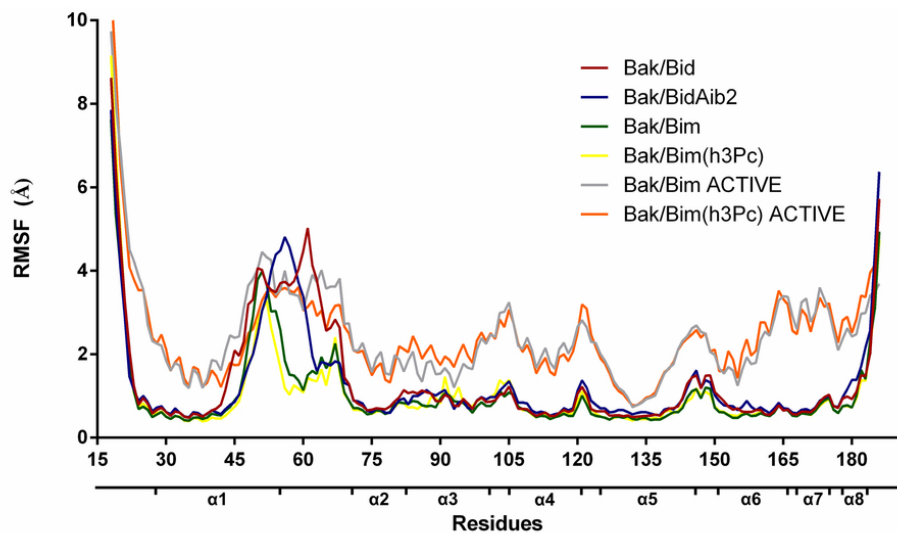


Figure 3: Average Root-Mean Square Fluctuation (\AA) from backbone atoms of three molecular dynamics simulations as a function of Bak residues in the complexes between Bak and BH3-only peptides. In red, Bak complex with Bid; in blue in complex with BidAib2; in green with Bim; and in yellow, Bim(h3Pc). Active conformations from Bim and Bim(h3Pc) are represented in grey and orange, respectively.

82x45mm (300 x 300 DPI)

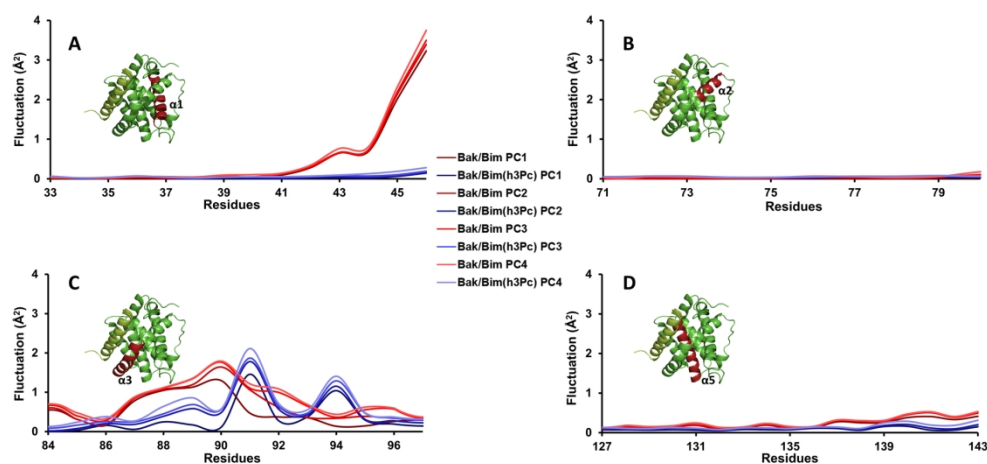


Figure 4: Principal Component Fluctuation (Å²) from Bak residues in the globular form. In red, fluctuation of Bak residues in complex with Bim, and in blue, fluctuation of Bak residues in complex with Bim(h3Pc). In both cases, each Principal Component (PC) illustrates the square summation of the PCs of residues and all the previous ones. (A) Square summation of all atoms fluctuation from helix α_1 . (B) Square summation of the fluctuation from all residues from helix α_2 . (C) Square summation of all residues fluctuation from helix α_3 . (D) Square summation of the fluctuation from all residues from helix α_5 .

170x82mm (300 x 300 DPI)

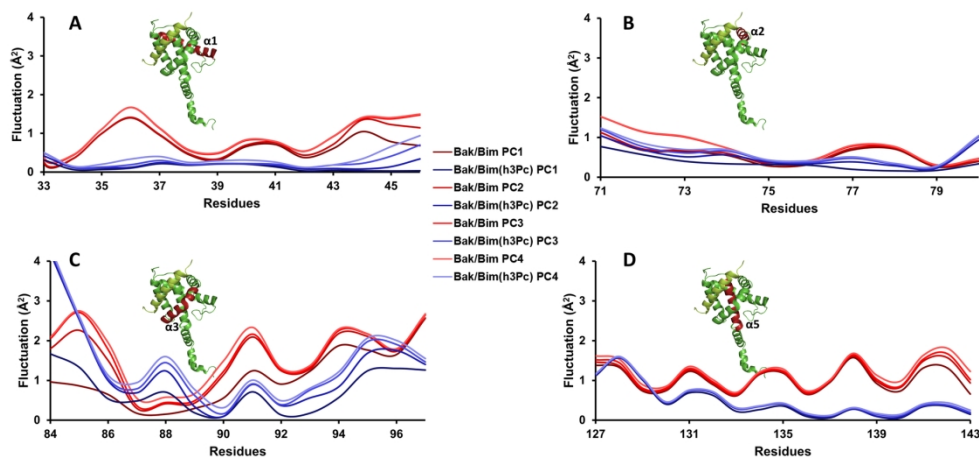


Figure 5: Principal Component Fluctuation (\AA^2) from Bak residues in the active conformations. In red, fluctuation of Bak residues in complex with Bim, and in blue, fluctuation of Bak residues in complex with Bim(h3Pc). In both cases, each Principal Component (PC) illustrates the square summation of the PCs of residues and all the previous ones. (A) Square summation of all atoms fluctuation from helix $\alpha 1$. (B) Square summation of the fluctuation from all residues from helix $\alpha 2$. (C) Square summation of all residues fluctuation from helix $\alpha 3$. (D) Square summation of the fluctuation from all residues from helix $\alpha 5$.

170x82mm (300 x 300 DPI)

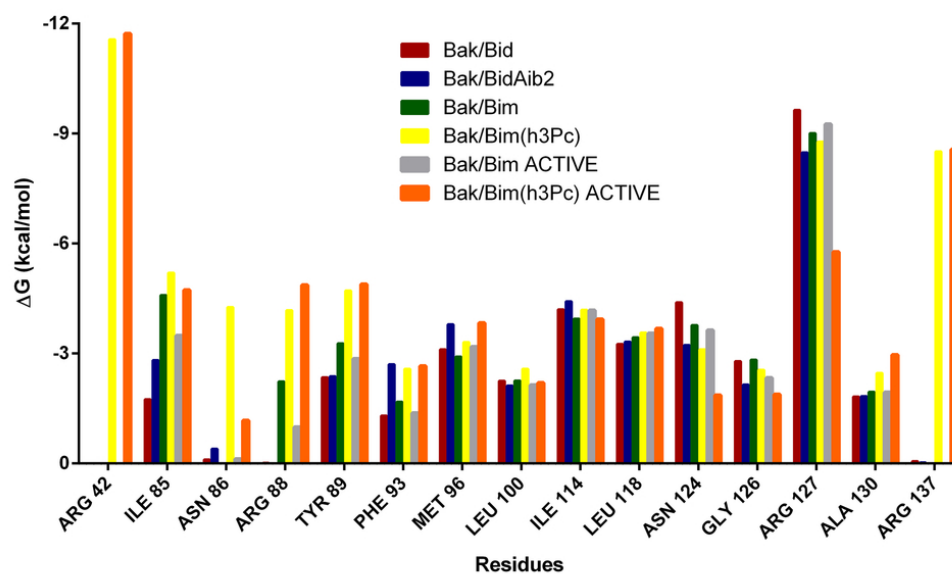


Figure 6: Average Total ΔG (kcal/mol) from Bak residues of three molecular dynamics simulations in the complexes between Bak and BH3-only peptides. In red, Bak complex with Bid; in blue, in complex with BidAib2; in green, with Bim; and in yellow, Bim(h3Pc). Active conformations from Bim and Bim(h3Pc) are represented in grey and orange, respectively.

82x52mm (300 x 300 DPI)

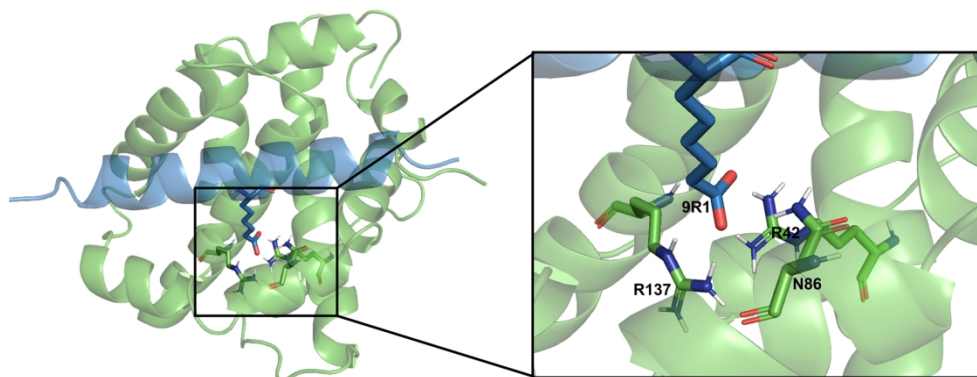


Figure 7: Interaction site from residue 9R1 155 from Bim(h3Pc). Pro-apoptotic protein Bak is represented in green and BH3 peptide Bim(h3Pc) in blue. Residues from Bak involved in the hydrogen bond with 9R1 are R42, N86 and R137.

170x66mm (300 x 300 DPI)

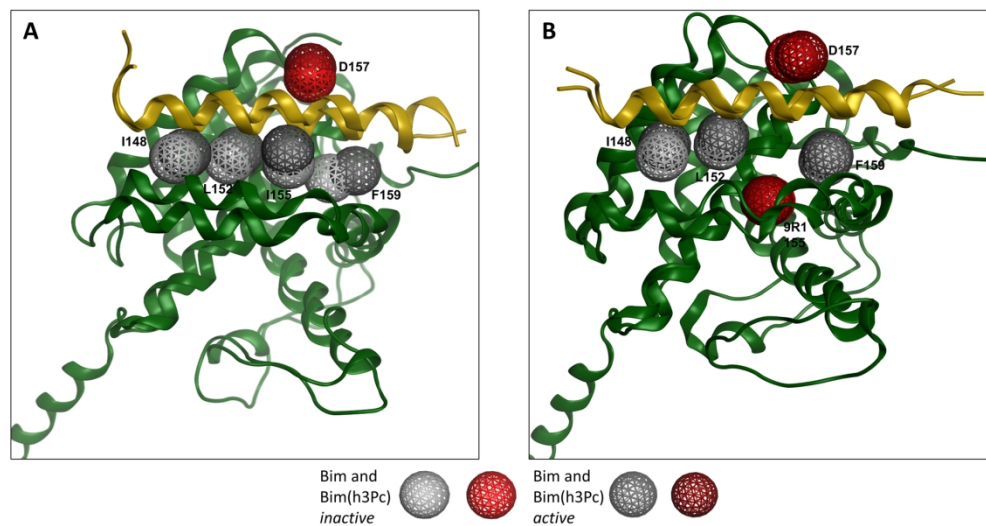


Figure 8: Pharmacophore representation of the interaction between Bak and BH3-only peptides Bim and Bim(h3Pc) on its inactive and active conformations. Light grey and light red are used for molecular features of the inactive conformations, while dark grey and dark red are used for features in the active conformations. (A) Comparison between Bak/Bim complexes on its inactive and active form. (B) Comparison between Bak/Bim(h3Pc) complexes on its inactive and active form.

170x92mm (300 x 300 DPI)